A major purpose of the Technical Information Center is to provide the broadest dissemination possible of information contained in DOE's Research and Development Reports to business, industry, the academic community, and federal, state and local governments.

Although a small portion of this report is not reproducible, it is being made available to expedite the availability of information on the research discussed herein.

1

LA-UR-84-264

CONF-840384--1

NOTICE

PORTIONS OF THIS REPORT ARE ILLEGIBLE.

It has been reproduced from the best available copy to permit the broadest possible availability.

Los Alamos National Laboratory is operated by the University of California for the United States Department of Energy under contract W-7405-ENG-36

LA-UR--84-254

DE84 006031

TITLE: DIGITAL HF RADAR OBSERVATIONS OF EQUATORIAL SPREAD-F

AUTHOR(S): Paul E. Argo

SUBMITTED TO: Seventh International Symposium on Equatorial Aeronomy
Hong Kong - March 22-29, 1984

Los Alamos

Los Alamos National Laboratory
Los Alamos, New Mexico 87545

Digital HF Radar Observations of Equatorial Spread-F

Paul E. Argo

Atmospheric Sciences Group
Earth and Space Sciences Division
Los Alamos National Labortory
Los Alamos, New Mexico 87545

Abstract

Modern digital ionosondes, with both direction finding and doppler capabilities can provide large scale pictures of the Spread-F irregularity regions. A morphological framework has been developed that allows interpretation of the HF radar data. A large scale irregularity structure is found to be nightward of the dusk terminator, stationary in the solar reference frame. As the plasma moves through this "foehn-wall-like" structure it descends, and irregularities may be generated. Localized upwellings, or bubbles, may be produced, and they drift with the background plasma. The spread-F irregularity region is found to be best characterized as a "partly cloudy" sky, due to the patchiness of the substructures.

Introduction

Since the first observations of Equatorial Spread-F (Booker and Wells, 1938), equatorial ionospheric irregularities have been studied using vertical incidence ionosondes, VHF radars, radio star and satellite scintillations, and various in situ techniques. Ionosondes have been used to provide long term statistics on spread-F, but have been too limited to make a major impact upon spread-F research (see reviews by Kelly and McClure, 1980; and Fejer and Kelley, 1980).

Modern digital ionosondes, with both echo direction finding and doppler capabilities (Wright and Pitteway, 1979, 1982) can provide large scale pictures of the spread-F irregularity regions. The mapping of localized regions of small scale irregularities, and their motion across the sky, indicate that digital sounders with direction finding (and doppler) capabilities are more useful during disturbed conditions than undisturbed, because during these disturbed periods echoes return from other than directly overhead and provide a more complete mapping of the sky.

This paper will discuss various aspects of Equatorial Spread-F data taken with the HF radar during the NASA sponsored "CONDOR" Spread-F campaign (March 1983). The HF radar was located at the Instituto de Geofysica, Huancayo Observatory, Huancayo, Peru (12:04°S latitude, 0.5°N dip). A morphology of the spread-F ionosphere will be provided as a framework for interpreting and understanding the present data.

I. General Morphology of Spread-F

Many reviews have been written on Equatorial Spread-F (Kelly and McClure, 1981; Fejer and Kelley, 1980; Ossakow, 1981) . We have used these reviews to shape a morphological frame work for the interpretation of the HF-radar observations which will be presented in this report. We will describe our interpretation of the equatorial spread-F morphology in a manner consistent with the radar data acquisition capabilities. In this sense this morphology is incomplete but we hope adequate to the task of interpreting the radar results.

1. Local Scenarios - bottomside spread F

In the post sunset F-layer the background plasma drift is generally eastward, at velocities of 100-200 m/s. In the first hours following sunset the F-layer (and its plasma) rise at 10-30 m/s. The layer bottom (identified as h_{min}) has risen from 200-250 kilometers altitude to greater than 300 kilometers (up to 500 km). Within one to three hours after sunset the layer (and plasma) begin to descend (again at 10-40 m/s) for several hours, until the layer bottom has returned to an altitude below ~250 kilometers.

As the layer descends bottomside irregularities may be generated along the descending portions. This irregularity generation is probably due to localized conditions, such as the vertical plasma density gradients. One criteria for the onset of irregularity formation appears to be the initial layer height--many observations indicate a threshold of ~340 km. Irregularities that have already been formed may survive after the layer drops below that threshold, however.

Bubbles/Plumes

As the plasma descends, and bottomside spread-F irregularities are generated, it is possible that nonlocally controlled conditions such as field line integrated conductivities, background acoustic gravity waves, etc. may produce "localized" upwellings--often called bubbles or plumes (Ossakow, 1981).

These upwellings carry the low density bottomside plasma up to and above the F-layer peak, creating a cavity of lower density plasma.

These upwellings or bubbles drift generally with the background plasma eastward at 100-200 m/s. They move therefore relative to the bottomside spread-F structure--and in fact have been observed completely detached (or isolated) from that structure (see Argo, 1984; Buchau et al. 1978).

2. Equatorial Spread-F from Various Reference Frames

Solar

The bottomside spread-F as a structure remains stationary in the solar reference frame, with the onset approximately one or two hours past sunset (Figs. 1 and 2). In this frame the bottomside spread-F appears as a pseudo-standing wave, with the onset very similar to the meteorological "foehn wall." The earth and plasma are rotating relative to the sun and so move by (or through) this structure with velocities of ~460 m/s (560^+ m/s for the plasma). The bubbles/plumes also drift relative to this structure.

Earth

The bottomside spread-F structure appears to move westward at ~460 m/s, and so a ground based observer will see this structure approach from the east (Fig. 3). The plasma drifts eastward at 100-200 m/s, and substructures such as bubbles will drift approximately with the plasma. Therefore, doppler measurements of the advancing front ("foehn wall") will show a receding velocity comparable to the plasma drift.

Plasma

In a reference frame stationary relative to the horizontal plasma drift, the observer would see plasma rising at 10-30 m/s, followed by a descending period (velocities of 10-30 m/s) (Fig. 4). Just following the onset of plasma descent the bottomside spread-F front ("foehn wall") would approach rapidly from the east (560^{+} m/s). In localized regions there would be upwelling plasma--these regions may or may not drift slowly eastward or westward.

3. Dynamic Structure Variations (Substructures and "clouds")

The previous morphological description has treated the bottomside spread-F structure as a non-changing feature in the post-sunset ionosphere. In fact, this structure has its own variations, and it will wax and wane with varying ionospheric conditions. On some nights observations indicate the complete lack of any measurable ionospheric irregularities.

If the bottomside spread-F structure is time varying, it may possibly not exist as its usual position approaches from the east, and may in fact be overhead or westward before bottomside spread-F begins. In this case a ground based ionosonde would observe the spread-F onset to the west, with all structures drifting eastward, overhead.

Another scenario may have a portion of the bottomside spread-F structure suitable for onset, but with local conditions above a ground based system such as to not support irregularity generation. In this case a ground based ionosonde might observe the "front" approach, but also observe it disappear before it arrives overhead--so no overhead spread-F would be observed on this given night.

In any case, inside the overall structure there will be a variety of substructures: the aforementioned upwellings or bubbles, regions of strong bottomside irregularities (generated from localized steep gradients), regions of no irregularity activity whatsoever, etc. In fact, as we see with the HF radar (and with spatial measurements from vhf radars; Tsunoda, 1981), the spread-F ionosphere is probably best characterized as a "partly cloudy" sky.

II. HF Radar Observations

1. Layer Motions and Spread-F Onsets

Many studies of spread-F onset have been performed in the past (e.g., Rastogi 1978; Sastri and Murthy, 1978). The term spread-F originated from the spread appearance of the F-region trace on ionograms. This spreading occurs as a result of the numerous returns received by an ionosonde during spread-F conditions. For the case of the standard ionosonde, it is not possible to remove the ambiguities arising in this multiple echo environment since the echoes may come from virtually anywhere in the sky. We have learned using the directional capability of the HF-radar that irregularity layers may approach from either the east (usually) or the west, and that these layers are seen when greater than 150 kilometers (and up to 1/2 hour) away.

Figure 5 shows the composite data for four evenings of observations, including three with overhead spread-F and one without. On each of the nights that we measured irregularities overhead, at the time the irregularities arrived overhead the layer was dropping rapidly ($12-20^{+}$ m/s). In two of these cases (March 9 14) the irregularity region approached from the east (although the measured Doppler velocity indicated an eastward irregularity drift). On the third night (March 13) the irregularity region was observed to the west at 0015 UT and the irregularities moved eastward until overhead at ~0130 UT. On each day when irregularities were observed to the east, the region appeared overhead in less than one half hour (mean velocities ~250^{+} m/s), whereas the one case with irregularities moving from the west took longer than one hour (mean velocity ~60 m/s) to arrive overhead.

The data presented is consistent with the picture developed in the general morphology section. The irregularities are generated locally when the layer is dropping. Subsequent rises do not damp out the irregularities, although they appear to grow less explosively - see March 8. When the irregularity structure first appears to the east it arrives overhead rapidly, albeit somewhat slower than the terminator velocity (460 m/s). When the irregularities appear to the west the arrival of the irregularities is much delayed--perhaps because they move at the plasma horizontal drift velocities.

With the framework developed in the morphology section, the initial appearance of irregularities to the west is interpreted as follows (see Fig. 6):

1) The conditions for irregularity generation are not met at the usual post-sunset time (1900-2000),
2) somewhat later the layer begins dropping--but now it is dropping in the west first,
3) irregularities develop--to the west--and drift overhead with the plasma,
4) spread-F (hence irregularity) activity proceeds as normal for remainder of evening.

An important point to keep in mind is that bottomside spread-F structure is nonstatic. Even in the solar frame it is dynamic--growing, shrinking, disappearing and reforming; only the general location remains situated behind the sunset terminator.

Layer height and spread-F Onset

Although the layer vertical motion is a controlling factor in the development of spread-F irregularities, the height of the layer is equally important. In the data discussed in the previous section the irregularity onset height was consistently above 340 km (h_{min} for the layer at overhead onset). On one of the seven evenings of observations there was no overhead spread-F--on this night the layer bottomside (h_{min}) never rose above ~310 kilometers (Fig. 5). An irregularity region was observed approaching from the east, but dissipated before arriving overhead.

2. Spread F Dynamics

Onset, Maturation, and Decay of the Irregularity Layer

The life cycle of the spread-F irregularity layer, as observed by the HF-radar, can be broken into three general stages: 1) onset, 2) maturation, and 3) decay.

Onset:

The onset of irregularities was observed following two general patterns. In one, the irregularity region moves overhead from the east, with local (overhead) onset occurring as the F-layer is dropping. The layer bottomside density gradient has "steepened," hence more easily supporting any gradient driven instabilities. During this period the irregularities affect primarily the lower HF frequencies (<4-5 MHz).

The other pattern appears very similar, except that the irregularity region has formed to the west and slowly drifts overhead.

Maturation:

As the irregularity layer remains overhead for longer than one half hour it appears to thicken (as it drops in altitude), and the spreading affects higher and higher frequencies (>5-7 MHz). It is during this stage that both frequency spread and complete spreading occur. Doppler contour maps (Fig. 7) indicate that the frequency (and complete) spreading is associated with large scale structures moving across the field of view (west-to-east). We believe that these structures are the often seen bubbles/plumes. Evidence of this is the near simultaneity of observation of such a structure by the HF radar, and observation of a plume by the Jicamarca VHF radar (Fig. 8).

Decay:

Eventually the horizontal extent of the measured irregularity region begins to decrease, and the high frequency structure in the ionograms disappears. The upper limit on the spread ionogram decreases until a quiet-time ionogram with solely overhead echoes remains.

Motion of Irregularity Region Substructures (Clouds)

Our morphology stressed the existence of a large scale stationary (at least in the solar reference frame) structure of ionospheric irregularities--through which the F-layer plasma flows. In fact, this large structure is not likely to be continuous, but rather will be made of medium scale (tens of kilometers) irregularity regions that are generated where localized conditions are optimum for irregularity growth. Evidence for these localized regions has previously been observed in spread-F ionograms (King, 1970), when inside the spread ionogram dominant traces have been recognized. In addition,using VHF radars Tsunoda (1981) has observed distinct patchiness in the bottomside irregularities. His data indicate that some of these patches preferentially are involved in the generation of the bubble/plume structures.

The HF-radar also observes these medium scale structures, drifting with the background plasma (west to east) see Fig. 9. When the echo location plots are treated as a time history movie these structures become very evident--the irregularity layer takes on the characteristics of time lapse cloud photography. There is continuous drift of structure on all scales across the radar field of view.

Bubbles/Plumes via Doppler Contour Maps

The region of irregularities associated with the bubble/plume should appear as a dominant feature of ionograms, and yet except for certain isolated structures (see next section) there have been no assertions that such features are seen. This is in part due to shortcomings in the standard ionosonde, in which echoes from all locations in the sky are mapped into a virtual range vs frequency picture--in essence losing all spatial information.

Comparison of HF radar data with the Jicamarca VHF radar data, as well as detailed analysis of the more complete HF radar ionograms does in fact show that ionosondes do observe the bubbles as they drift by. Bubbles (or plumes) have been shown by Tsunoda (1981) to be regions of electron density depletion (as predicted theoretically by Zalezak and Ossakow, 1980). Ionosondes observe plasma depletion regions as structure (or spread) at the upper frequencies of the ionogram (Paul, et al., 1968); therefore we might expect evidence for ionospheric bubbles/plumes to be evidenced at the nose of the ionogram. This is in fact the case, Fig. 10 shows ionograms taken at the time JRO observes plume structures. By isolating the high frequency echoes, and mapping the time evolution of their motion, a region of irregularities is found to drift west-to-east. It is this region that is associated with the bubble/plume.

The HF radar estimates line of sight Doppler for each returned echo by measuring returned echo phase changes for closely spaced pulses (see more complete description in Argo, 1984). By averaging these doppler measurements over horizontal regions of ~25 kilometer extent velocity distributions can be obtained (Fig. 7). If the observed distributions are stacked in 25 kilometer wide sections (extending east/west, with altitudes 200-500 km), a spatial picture of spread-F can be developed. During quiet times, only the regions directly overhead yield returns; but as irregularity regions drift through the sky, large scale patterns develop. Figure 7 is a contour map of the post sunset spread-F of March 14, 1983. This day was chosen due to the availability of simultaneous data with JRO. Note that as a plume develops in the VHF data (0200 UT, 2200 LT), a large-scale structure is drifting through the contour map. These structures are evident on all nights of spread-F activity. Figure 11 a,b show two more evenings of doppler contour maps. Unfortunately, on these nights no F-layer data from JRO is available for comparison and verification of plume identification.

3. Isolated or Detached Structures

Ionosondes have indicated the presence of F-layer structures in the post-midnight ionosphere (Buchau, et al. 1978). The HF radar also has documented the presence of such structures on at least three occasions. On two of these occasions the structures were observed to move from west to east, with velocities of 150 m/sec and 65 m/sec (see Argo, 1984). In both cases, the ionograms showed the characteristic features of frequency spreading. The high frequencies were affected first, with lower frequencies affected as the regions moved overhead (figure 12). Investigations of manmade depletions show ionograms remarkably similar to these (Paul, et al., 1968) - the conclusion is that the drifting regions contain underdense plasma, much as a bubble/plume would.

The most notable feature of these structures is the apparent lack of connection to any bottomside irregularities. Either they are bubbles generated earlier in the evening that have outlasted their underlying generation mechanism, or they are following an unseen energy source. Tsunoda (1981) estimates plume decay rates of 5-18 dB per ten minutes for one meter scale size irregularities. At this decay rate clearly no one meter irregularities would remain from the post-sunset bubbles. Buchau et al. (1978) show the co-existence of three meter irregularities (JRO) with their isolated region - we unfortunately have no such simultaneous data.

Although the overall west to east motion of the 0600 UT March 8 irregularity region is found to be 65 m/sec (figure 13), the doppler measurements indicate a reduced horizontal velocity of between 100 and 240 m/sec (depending on assumptions made). The doppler is obtained from individual reflections within the region, so this result indicates that the small scale irregularities are moving at 2-4 times the velocity of the overall structure.

In the early morning of March 15 (local date), the radar observed a structure appear to the west, remain 200 kilometers away for almost one hour, and then disappear. The local time for this event was 0500-0600 (just predawn), near the time of plasma drift reversal. In this case a very late isolated structure may have approached from the west, been stopped by the drift reversal, and either moved out of the radar field of view or dissipated altogether.

III. Conclusions

A general morphology of spread-F, in which the structure is stationary in a solar reference frame (hence moving in the earth and plasma reference frames), provides a coherent framework for interpreting the HF radar data. Although the horizontal motion is constant and eastward (~100 m/sec) at sunset, the plasma moves upward, and then downward. Along the downward section localized conditions (such as vertical plasma density gradients) are proper for irregularity generation. Hence small (~ tens of kilometers) regions of bottomside irregularities are produced that drift eastward, generally with the plasma drift. In addition, nonlocal (yet isolated) conditions (e.g. field line integrated conductivities) may produce "localized" upwellings or bubbles. These upwellings, which become plasma density depletions, also drift approximately with the plasma drift. In fact, the spread-F ionosphere is best characterized as a "partly cloudy" sky.

The HF-radar can provide information on irregularity onset, as well as subsequent motion of the irregularity structures. In the past, ionosonde observations have been interpreted as indicating that spread-F irregularities may onset with the F-layer either rising or falling. The HF radar observations show that although echoes from irregularities may be present on an ionogram during the layer rise, these echoes are from a distance of greater than 150 kilometers horizontal distance. In fact, in all cases as irregularities moved overhead the layer (overhead) was descending. This fact is important in assessing generation mechanisms.

In addition, irregularity onset usually included irregularities from the east, with the structure moving rapidly westward; occasionally the echoes indicate that irregularity onset is to the west, with the structure following the plasma drift eastward. The second case is interpreted as the result of changes in the usual structure of the spread-F region.

Although the plume/bubble is difficult to observe in an individual ionogram, detailed processing of time series of HF radar ionograms does show large scale structures moving from west to east. One night of simultaneous Jicamarca VHF radar data and HF radar data has led to tentative identification of these structures with the previously observed plumes or bubbles. In fact, the HF radar has observed isolated or detached structures in the post-midnight ionosphere that have many characteristics of bubbles. These structures are detached in the sense that there is no bottomside spread-F during the transit of the structure.

Acknowledgements

I would like to acknowledge the invaluable assistance of Kurt Moore of the Computer Support Group, Earth and Space Sciences Division, Los Alamos National Laboratory and J. W. Wright of CIRES, University of Colorado in the experimental data collection. The logistics support of the Peruvian Instituto de Geofysica, and CONIDA, made the experiment possible; the hospitality of Jean and Madeline Lanat made it enjoyable. In addition, many valuable discussions with my colleagues at Los Alamos (David Simons, Dwight Rickle, John Wolcott, Lewis Duncan and Paul Bernhardt) were instrumental in leading to the above picture of the Spread-F phenomena.

REFERENCES

Argo, P. E., "The Equatorial Spread-F of March 8, 1983," in preparation.

Booker, H. G. and H. W. Wells, "Scattering of Radio Waves by the F-Region of the Ionosphere," Terr. Magn. Atmos., Electr., 43, 249, 1938.

Buchau, J., E. J. Weber and J. P. McClure, "Radio and Optical Diagnostics Applied to an Isolated Equatorial Scintillation Event," in Effect of the Ionosphere on Space and Terrestrial Systems, edited by J. M. Goodman, p.115, U.S. Government Printing Office, Washington, D.C., 1978.

Fejer, B. and M. C. Kelley, "Ionospheric Irregularities," Rev. Geophys. Space Res., 18, 401, 1980.

Kelley, M. C. and J. P. McClure, "Equatorial Spread-F: A Review of Recent Experimental Results," J. Atmos. Terr. Phys., 43, 427, 1981.

King, G. A. M., "Spread-F on Ionograms," J. Atmos. Terr. Phys., 32, 209, 1970.

Ossakow, S. L., "Spread-F Theories - A Review," J. Atmos. Terr. Phys., 43, 437, 1981.

Paul, A. K., G. H. Smith and J. W. Wright, "Ray-Tracing Synthesis of Ionogram Observations of a Large Local Disturbance in the Ionosphere," Radio Science, 3, 15, 1968.

Rastogi, R. G., "On the Equatorial Spread F," Proc. Indian Acad. Sci., 87, 115, 1978.

Sastri, J. H. and B. S. Murthy, "On the Onset of Equatorial Spread-F," Ann. Geophys., 34, 47, 1978.

Tsunoda, R. T., "Time Evolution and Dynamics of Equatorial Backscatter Plumes, 1. Growth Phase," J. Geophys. Res., 86, 139, 1981.

Wright, J. W., and M. L. V. Pitteway, "Real-time Data Acquisition and Interpretation Capabilities of the Dynasonde, 2. Determination of Magnetoionic Mode and Echo Location Using a Small Spaced Receiving Array," Radio Science, 14, 827, 1979.

Zalesak, S. T., and S. L. Ossakow, "Nonlinear Equatorial Spread-F: Spatially Large Bubbles Resulting from Large Horizontal Scale Initial Perturbations," J. Geophys. Res., 86, 2131, 1980.

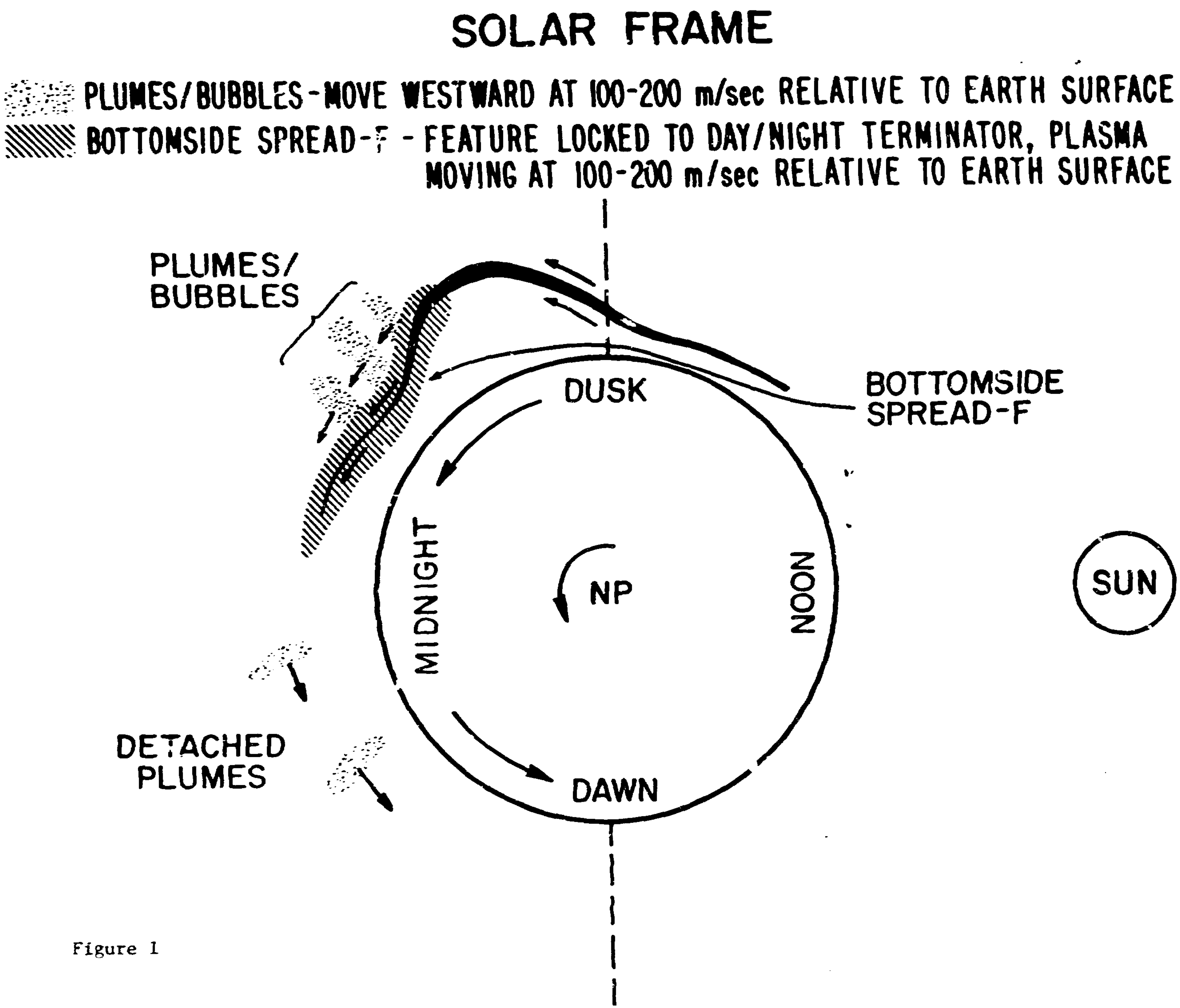
SOLAR FRAME
PLUMES/BUBBLES - MOVE WESTWARD AT 100-200 m/sec RELATIVE TO EARTH SURFACE
BOTTOMSIDE SPREAD-F - FEATURE LOCKED TO DAY/NIGHT TERMINATOR, PLASMA MOVING AT 100-200 m/sec RELATIVE TO EARTH SURFACE
PLUMES/ BUBBLES
BOTTOMSIDE SPREAD-F
DUSK
MIDNIGHT
NP
NOON
SUN
DAWN
DETACHED PLUMES

Figure 1

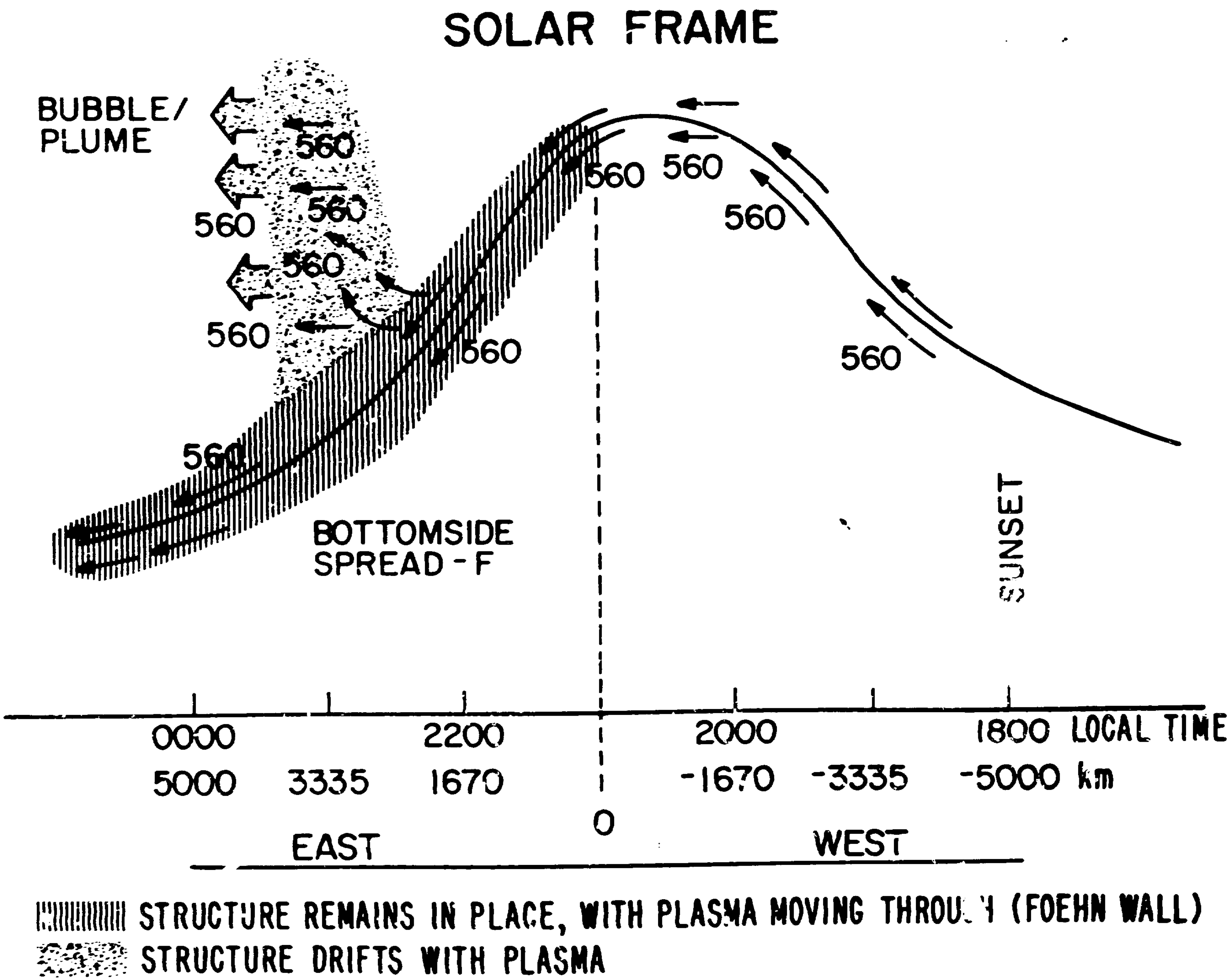
SOLAR FRAME
BUBBLE/
PLUME
560
560
560
560
560
560
560
560
560
560
560
560
560
BOTTOMSIDE
SPREAD - F
SUNSET
0000
2200
2000
1800
LOCAL TIME
5000
3335
1670
-1670
-3335
-5000 km
0
EAST
WEST
STRUCTURE REMAINS IN PLACE, WITH PLASMA MOVING THROUGH (FOEHN WALL)
STRUCTURE DRIFTS WITH PLASMA

Figure 2

EARTH FRAME

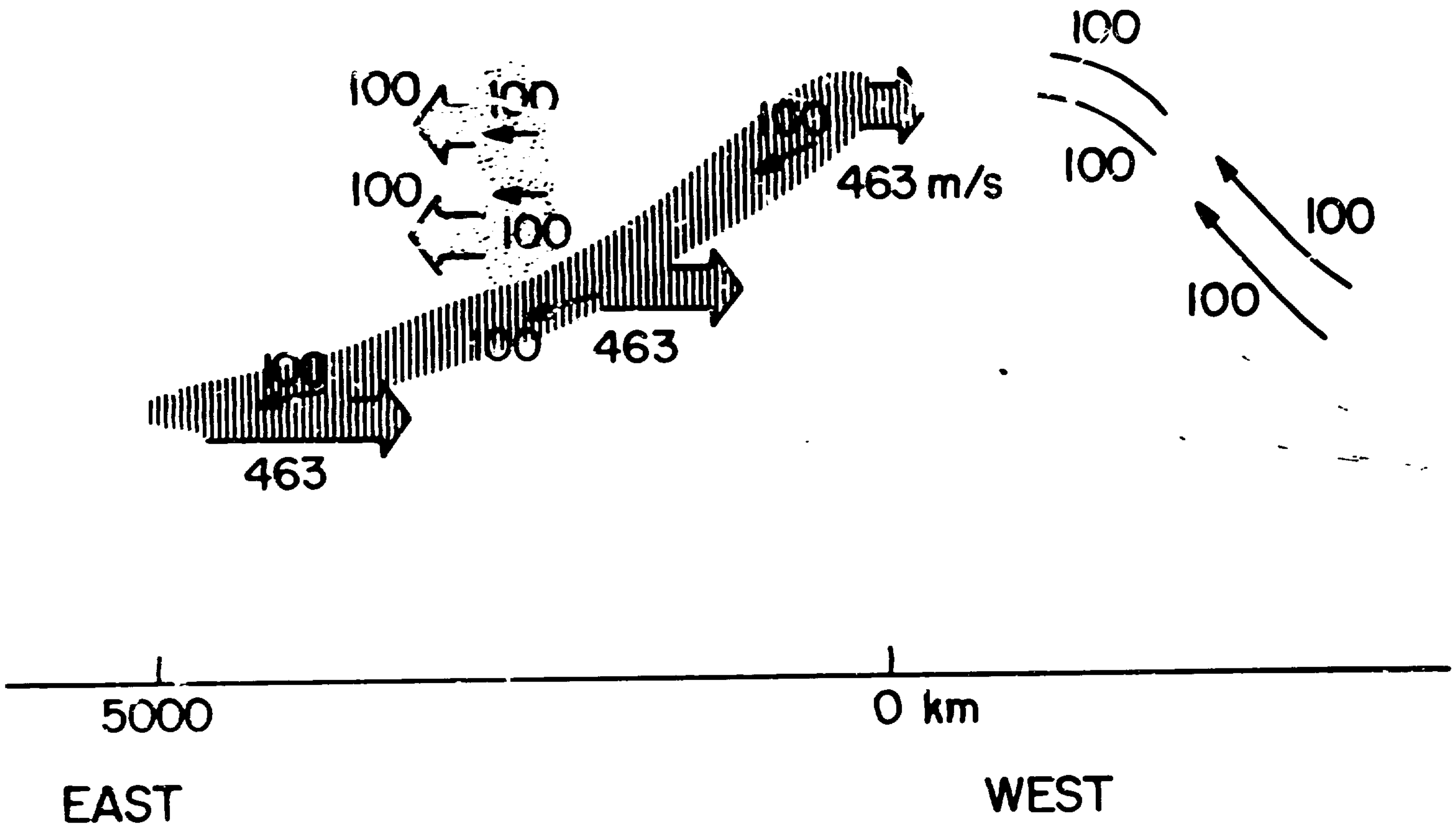

Figure 3

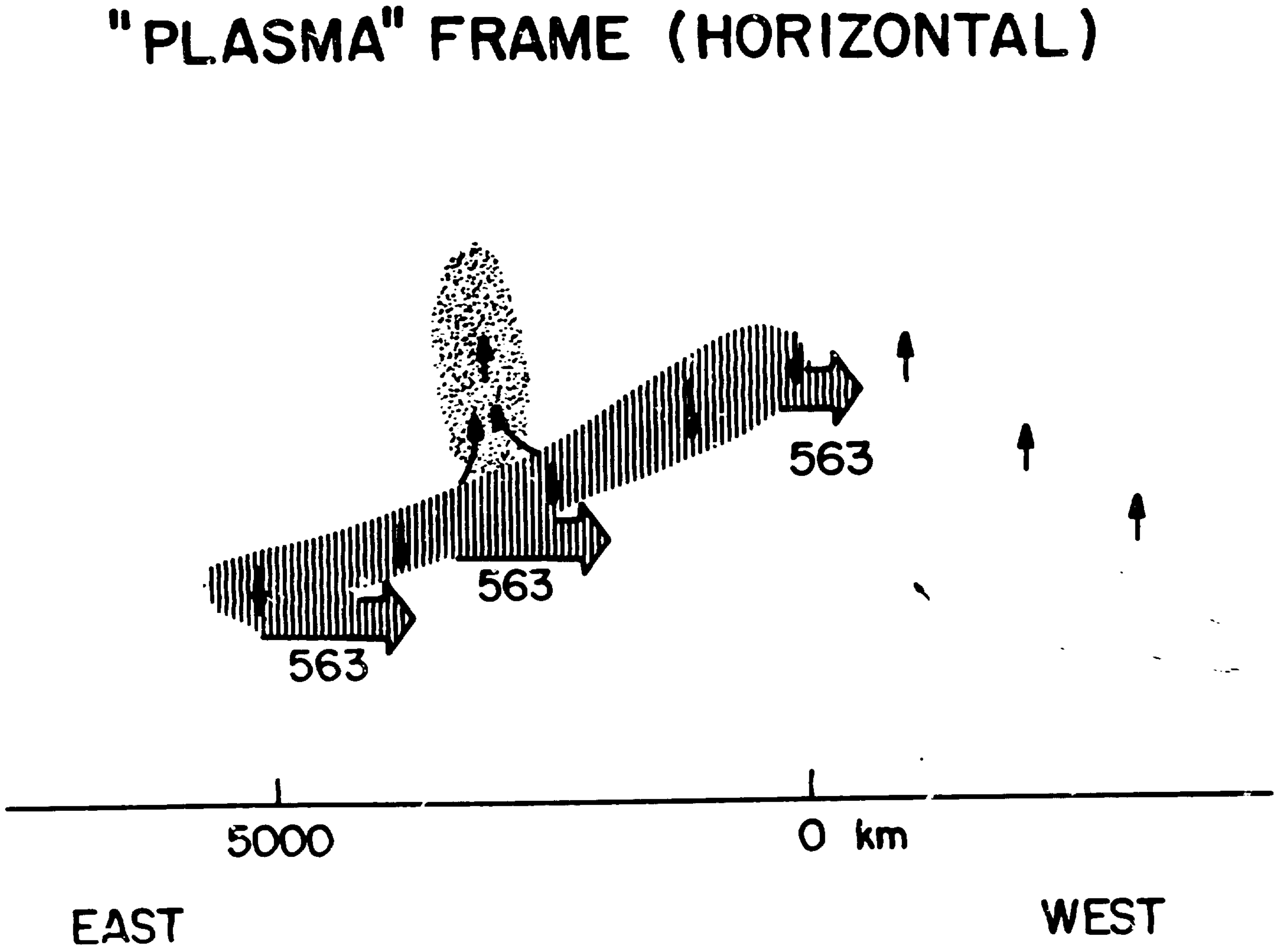

Figure 4

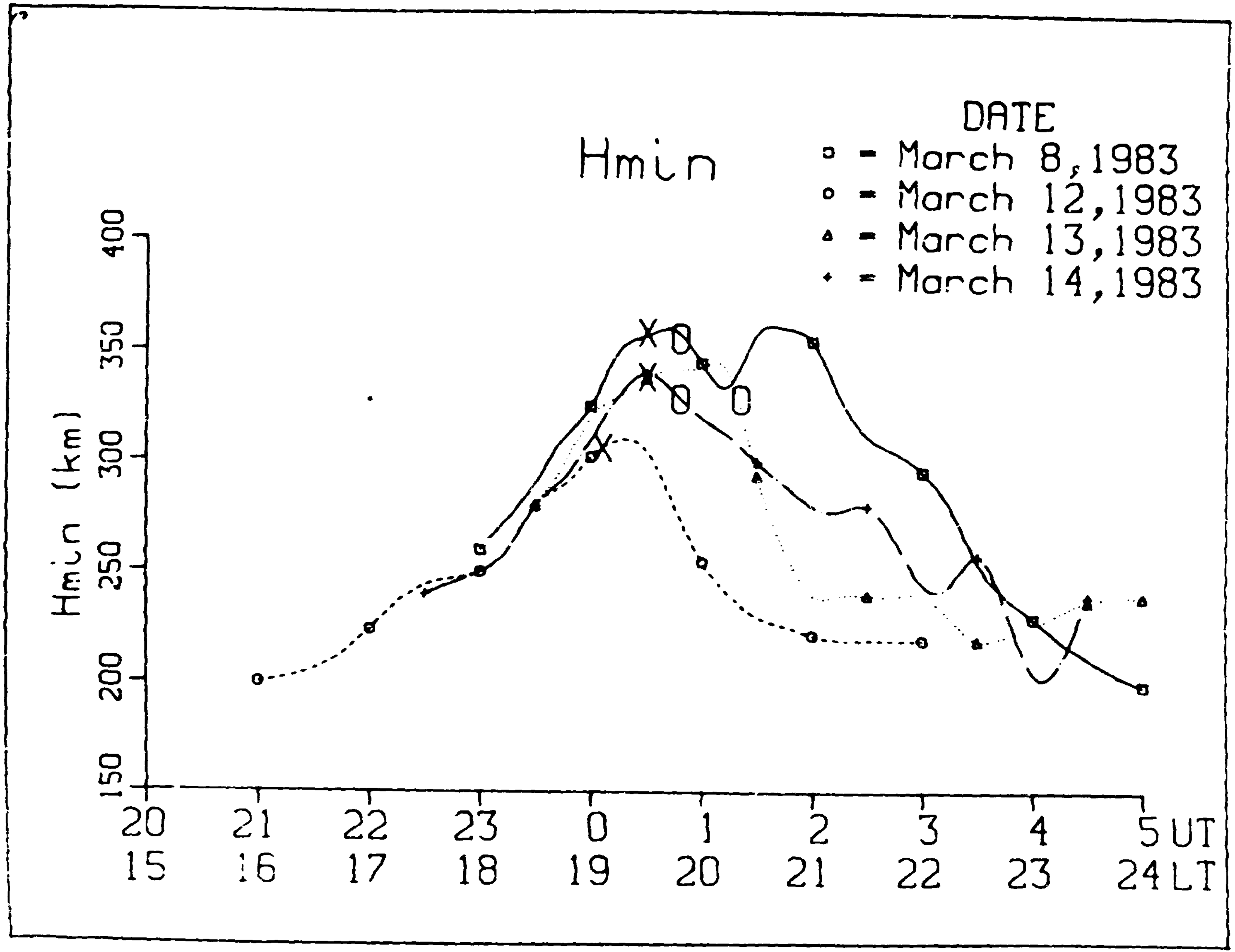

Hmin
DATE
□ = March 8,1983
○ = March 12,1983
△ = March 13,1983
+ = March 14,1983
Hmin (km)
400
350
300
250
200
150
20 21 22 23 0 1 2 3 4 5 UT
15 16 17 18 19 20 21 22 23 24 LT

Figure 5

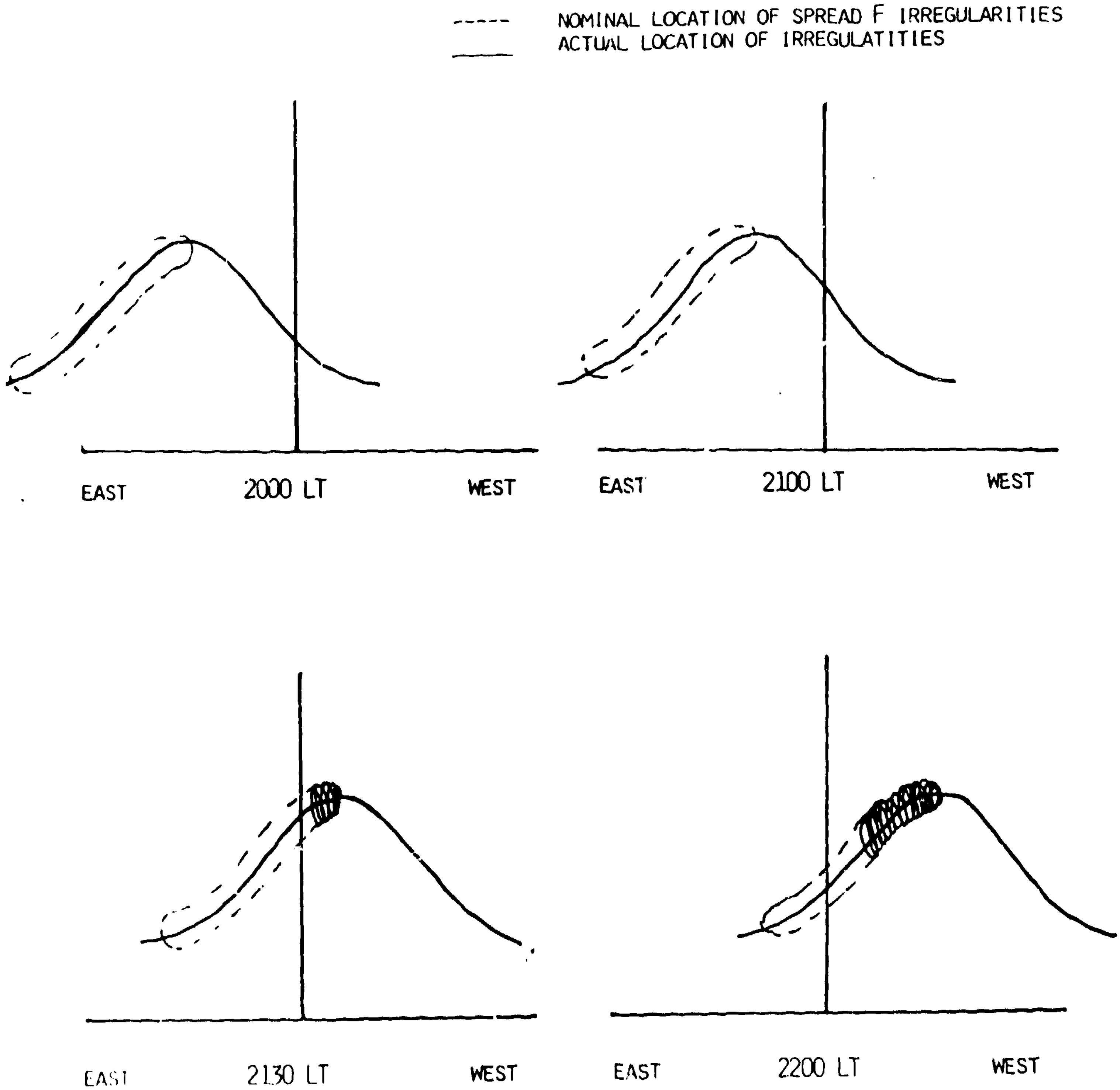
NOMINAL LOCATION OF SPREAD F IRREGULARITIES
ACTUAL LOCATION OF IRREGULATITIES
EAST
2000 LT
WEST
EAST
2100 LT
WEST
EAST
2130 LT
WEST
EAST
2200 LT
WEST

Figure 6

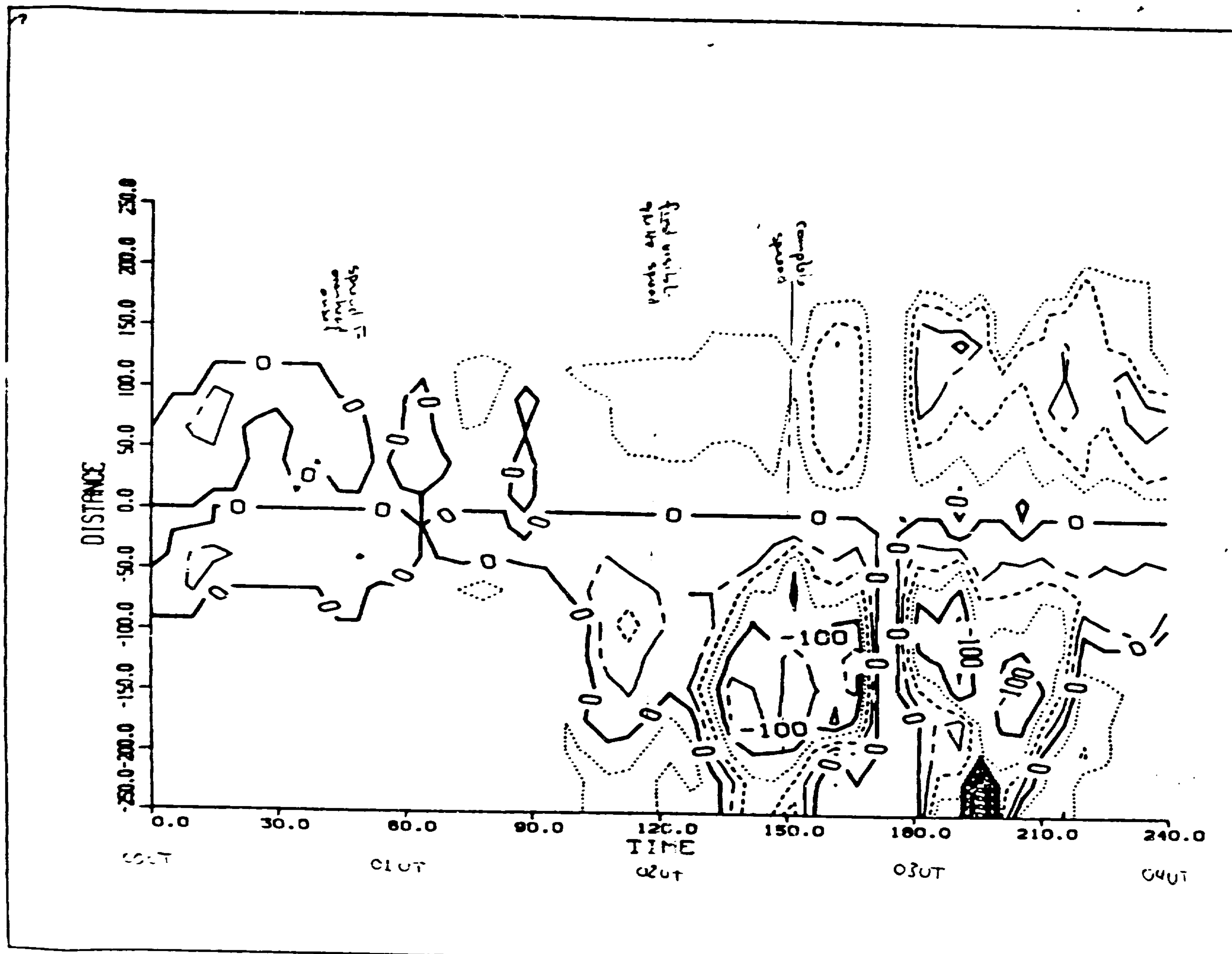
DISTANCE
250.0
200.0
150.0
100.0
50.0
0.0
-50.0
-100.0
-150.0
-200.0
-250.0
TIME
0.0
30.0
60.0
90.0
120.0
150.0
180.0
210.0
240.0
01UT
02UT
03UT
04UT
-100
-100
0

Figure 7

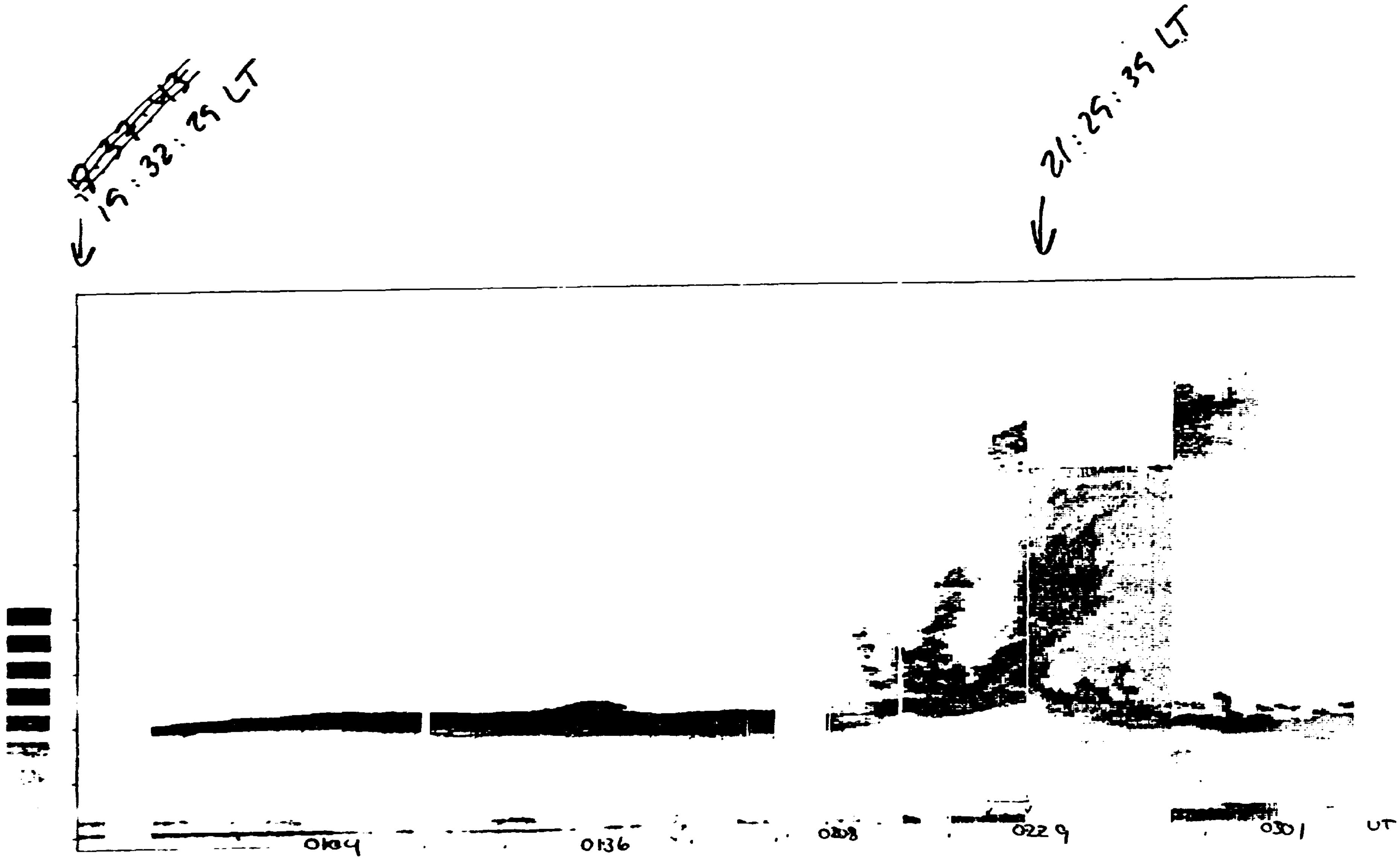

Figure 8

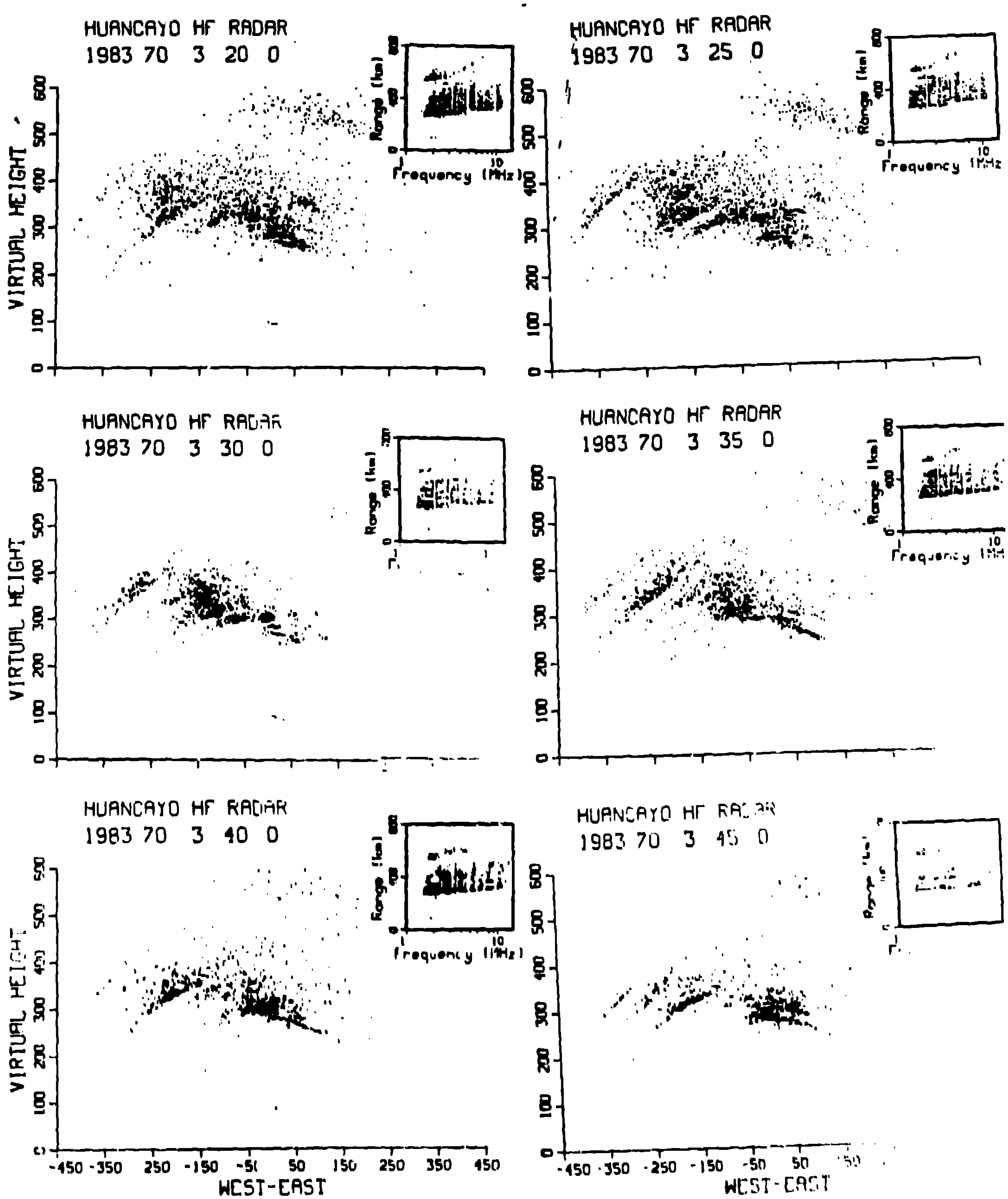
HUANCAYO HF RADAR
1983 70 3 20 0
HUANCAYO HF RADAR
1983 70 3 25 0
HUANCAYO HF RADAR
1983 70 3 30 0
HUANCAYO HF RADAR
1983 70 3 35 0
HUANCAYO HF RADAR
1983 70 3 40 0
HUANCAYO HF RADAR
1983 70 3 45 0
VIRTUAL HEIGHT
WEST-EAST
Range (km)
Frequency (MHz)

Figure 9

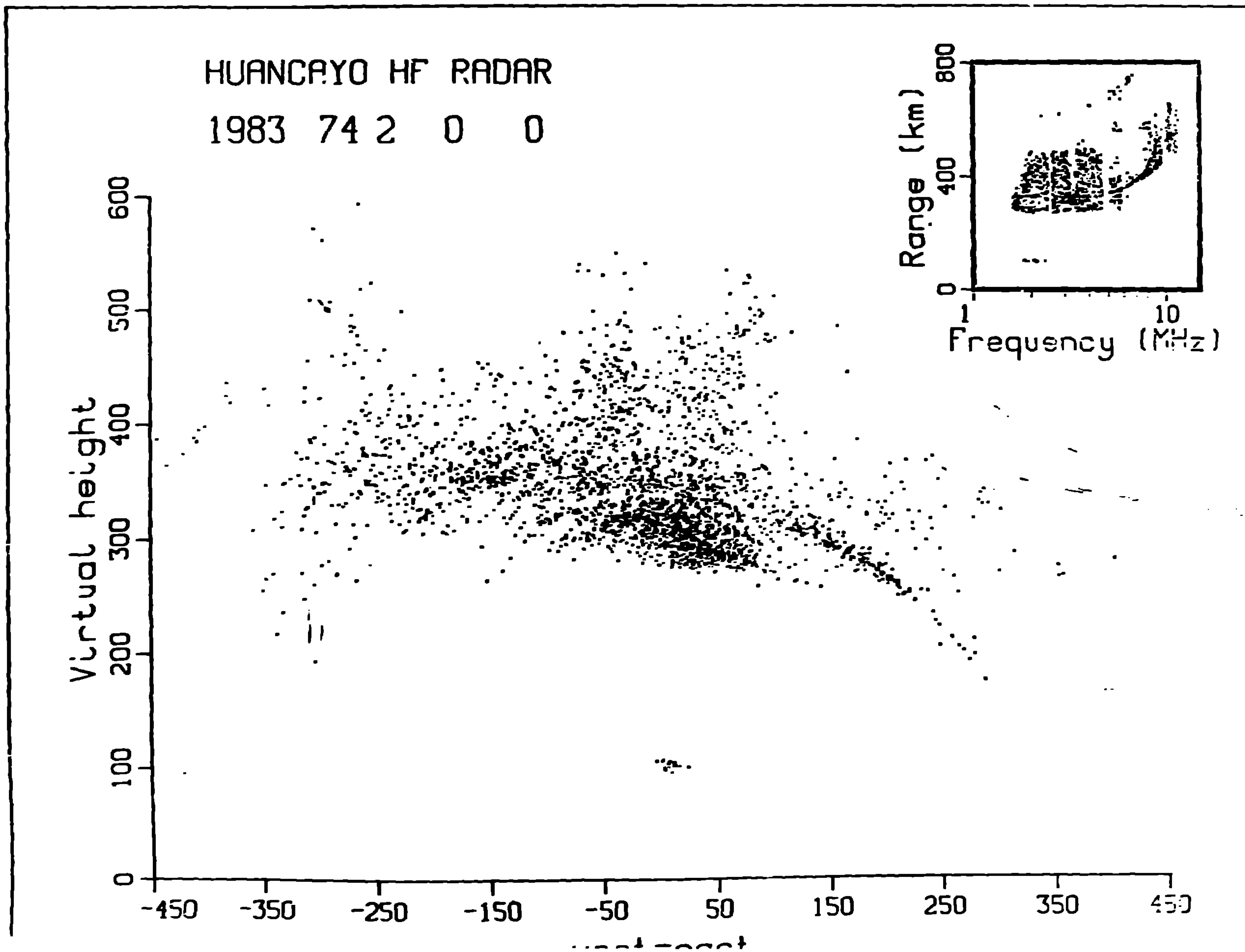
HUANCAYO HF RADAR
1983 74 2 0 0
Virtual height
0
100
200
300
400
500
600
-450
-350
-250
-150
-50
50
150
250
350
450
Range (km)
0
400
800
1
10
Frequency (MHz)

Figure 10a

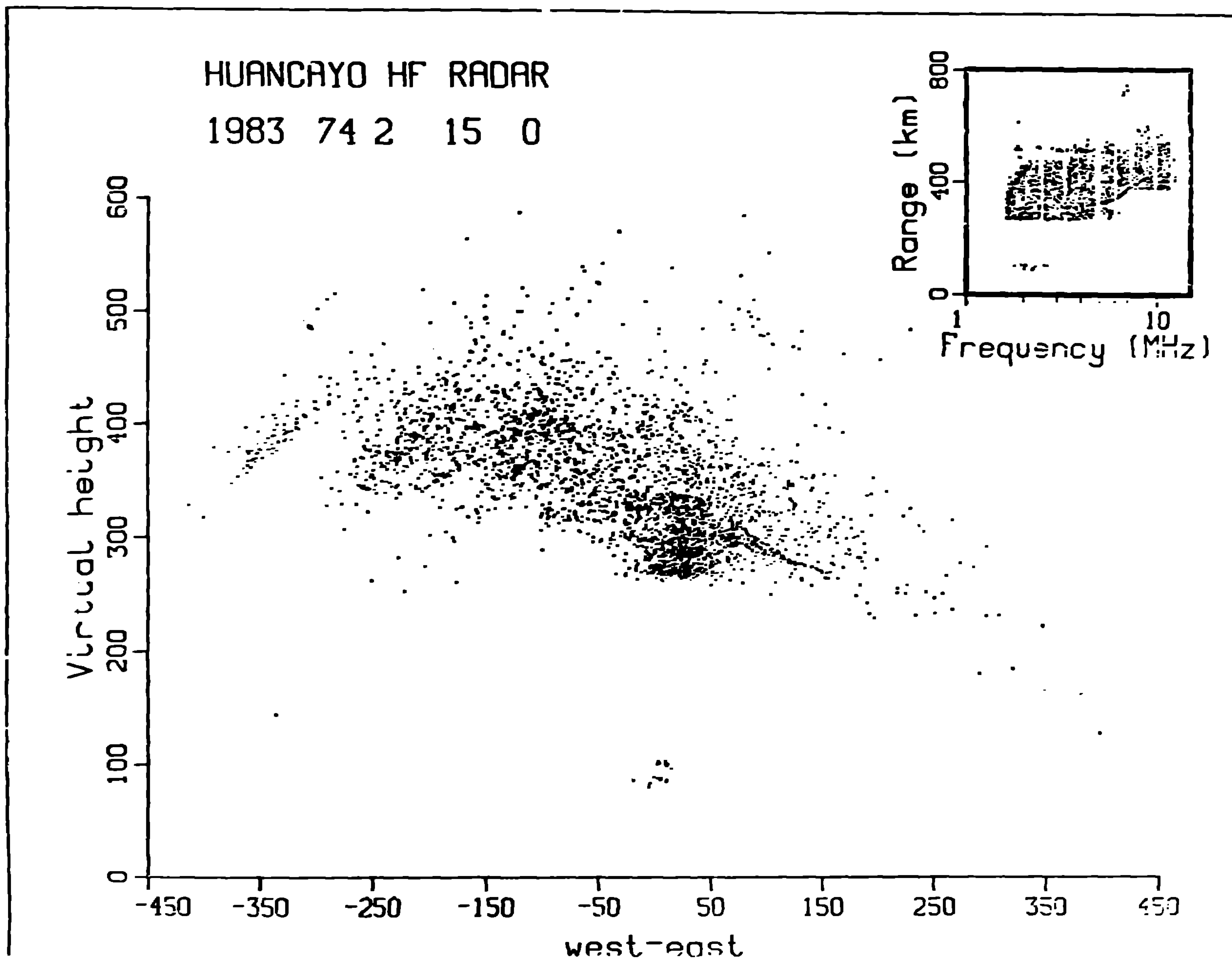
HUANCAYO HF RADAR
1983 74 2 15 0
Virtual height
west-east
0
100
200
300
400
500
600
-450
-350
-250
-150
-50
50
150
250
350
450
Range (km)
0
400
800
1
10
Frequency (MHz)

Figure 10b

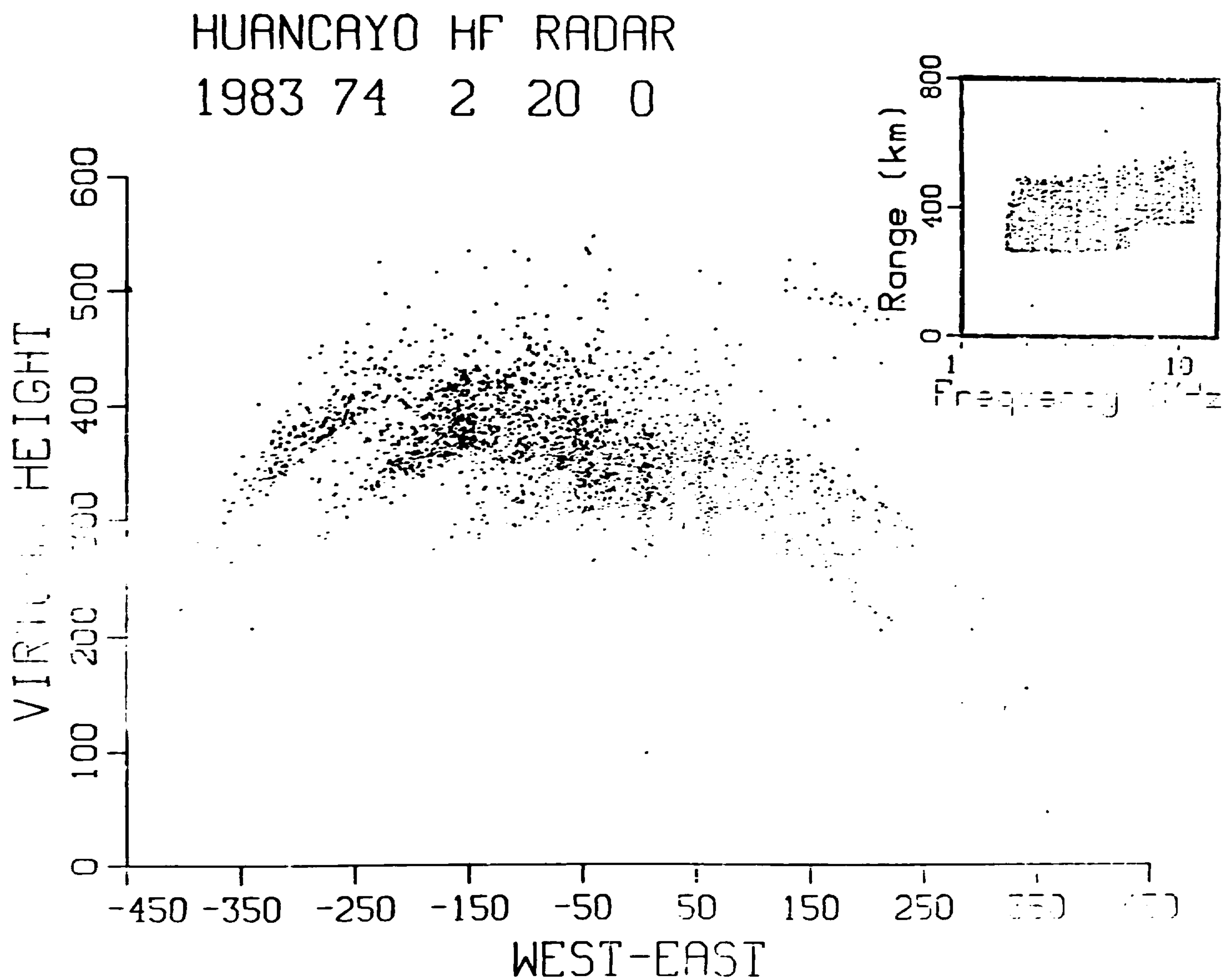
HUANCAYO HF RADAR
1983 74 2 20 0
VIRTUAL HEIGHT
600
500
400
200
100
0
-450 -350 -250 -150 -50 50 150 250
WEST-EAST
Range (km)
800
400
0
1
10

Figure 10c

Figure 11a

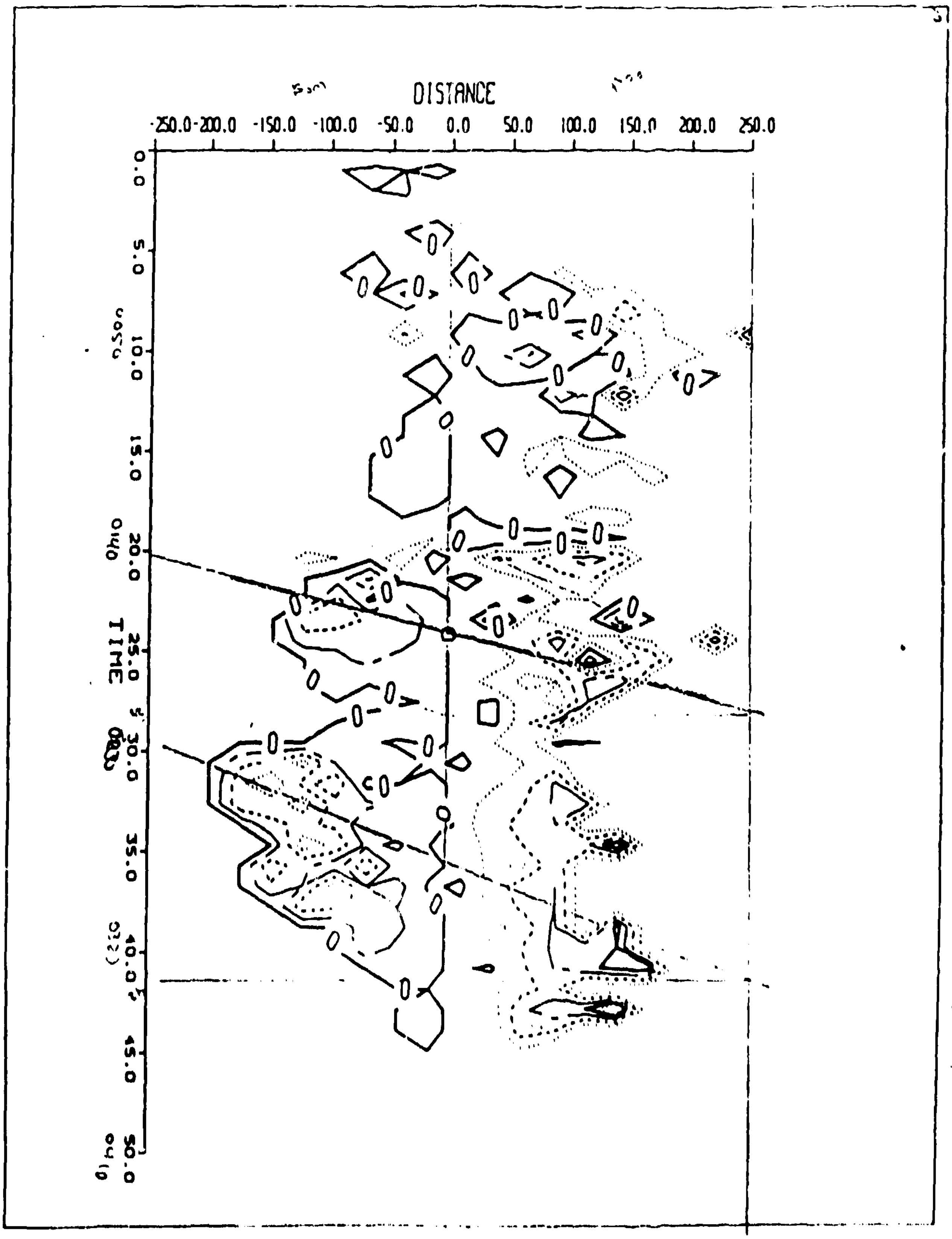
DISTANCE
-250.0 -200.0 -150.0 -100.0 -50.0 0.0 50.0 100.0 150.0 200.0 250.0
TIME
0.0 5.0 10.0 15.0 20.0 25.0 30.0 35.0 40.0 45.0 50.0

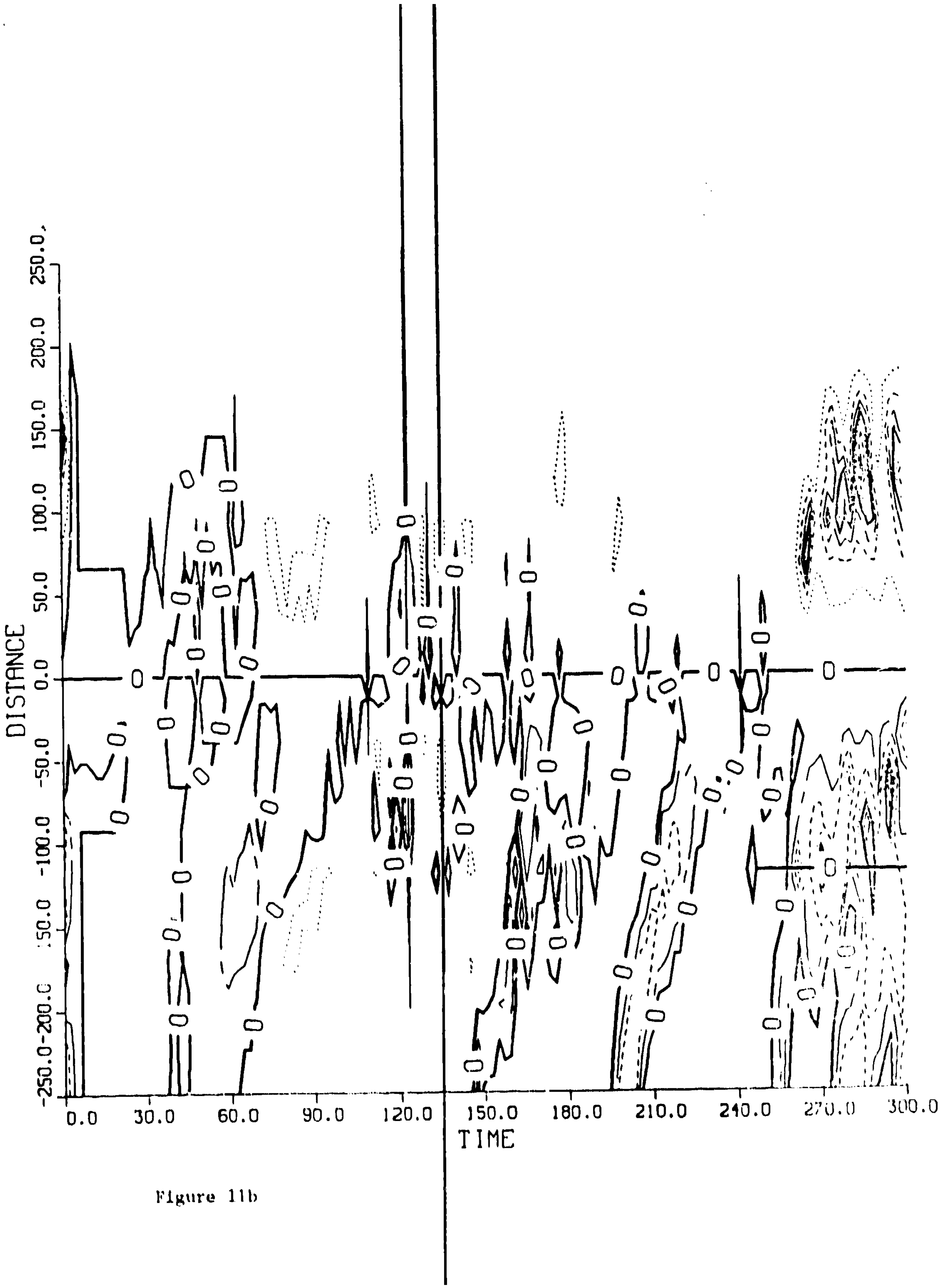

Figure 11b

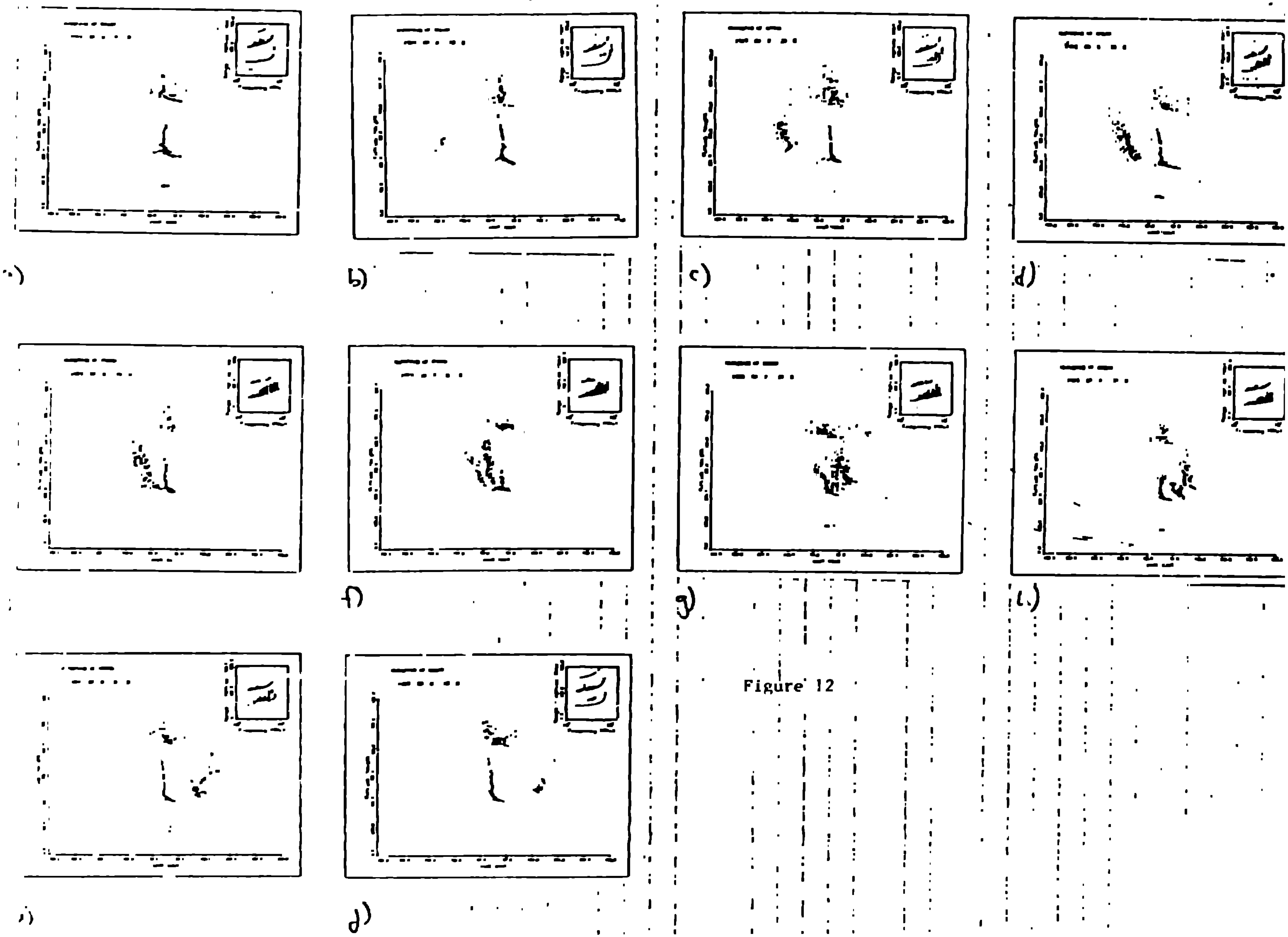

Figure 12

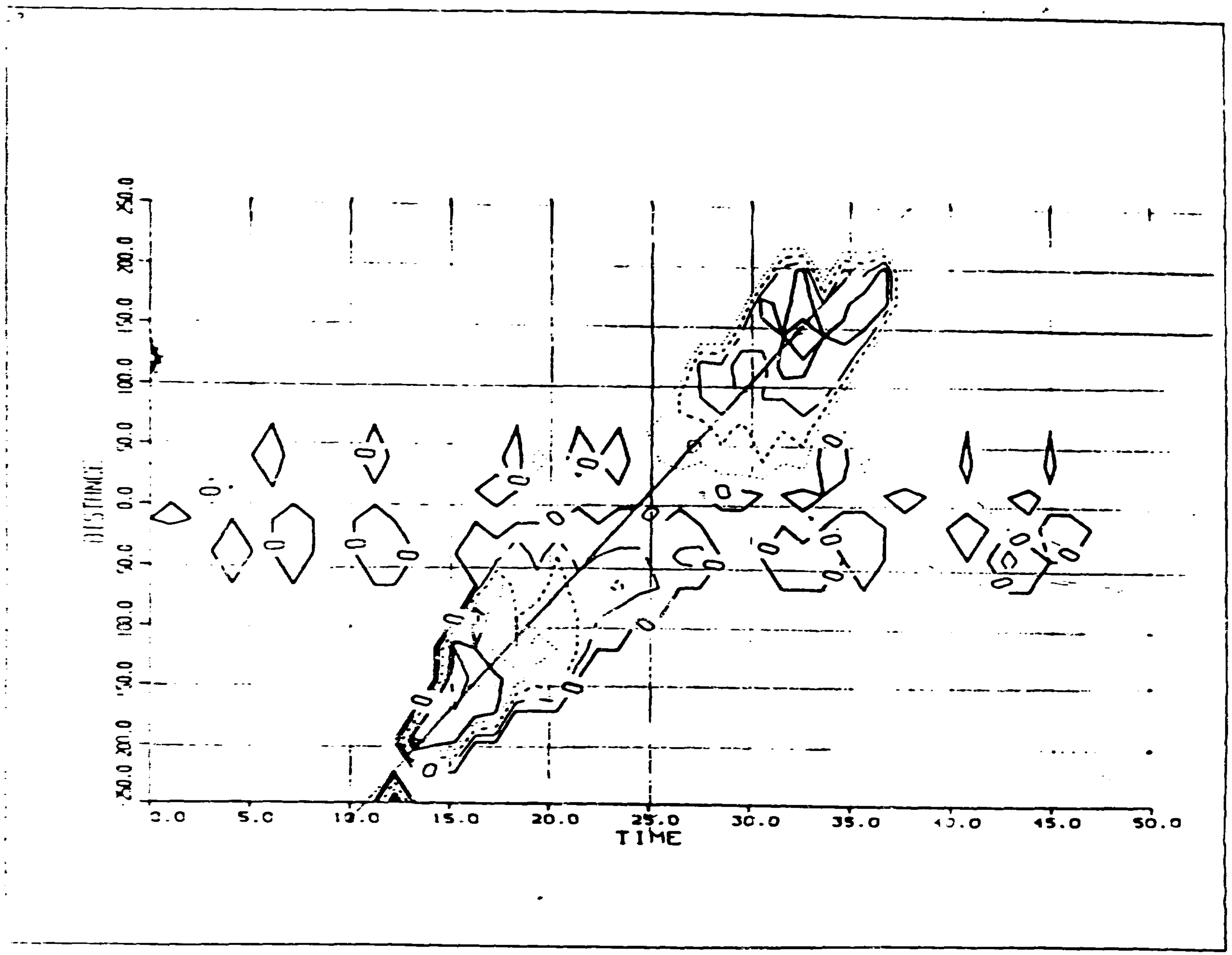
DISTANCE
250.0
200.0
150.0
100.0
50.0
0.0
50.0
100.0
150.0
200.0
250.0
0.0
5.0
10.0
15.0
20.0
25.0
30.0
35.0
40.0
45.0
50.0
TIME

Figure 13